

# Heavy quark spin multiplet structure of $P_c$ -like pentaquark as P-wave hadronic molecular state

Yuki Shimizu,<sup>1,\*</sup> Yasuhiro Yamaguchi,<sup>2,†</sup> and Masayasu Harada<sup>1,‡</sup>

<sup>1</sup>*Department of Physics, Nagoya University, Nagoya 464-8602, Japan*

<sup>2</sup>*Theoretical Research Division, Nishina Center, RIKEN, Hirosawa, Wako, Saitama 351-0198, Japan*

(Dated: January 29, 2019)

We study the heavy quark spin (HQS) multiplet structure of P-wave  $Q\bar{Q}qqq$ -type pentaquarks treated as molecules of a heavy meson and a heavy baryon. We define the light-cloud spin (LCS) basis decomposing the meson-baryon spin wavefunction into the LCS and HQS parts. Introducing the LCS basis, we find HQS multiplets classified by the LCS; five HQS singlets, two HQS doublets, and three HQS triplets. We construct the one-pion exchange potential respecting the heavy quark spin and chiral symmetries to demonstrate which HQS multiplets are realized as a bound state. By solving the coupled channel Schrödinger equations, we study the heavy meson-baryon systems with  $I = 1/2$  and  $J^P = (1/2^+, 3/2^+, 5/2^+, 7/2^+)$ . The bound states which have same LCS structure are degenerate at the heavy quark limit, and the degeneracy is resolved for finite mass. This HQS multiplet structure will be measured in the future experiments.

## I. INTRODUCTION

In 2015, the Large Hadron Collider beauty experiment (LHCb) collaboration observed two hidden charm pentaquarks,  $P_c^+(4380)$  and  $P_c^+(4450)$  [1–3]. Their masses are  $M_{P_c(4380)} = 4380 \pm 8 \pm 28$  MeV and  $M_{P_c(4450)} = 4449.8 \pm 1.7 \pm 2.5$  MeV, and decay widths are  $\Gamma_{P_c(4380)} = 205 \pm 18 \pm 86$  MeV and  $\Gamma_{P_c(4450)} = 39 \pm 5 \pm 19$  MeV. Their spin and parity are not determined. The one state has  $J = 3/2$  and the other has  $J = 5/2$  and their parity is opposite.

The  $P_c$  pentaquarks have a charm quark and an anti-charm quark. They are called the hidden-charm pentaquarks. There were some theoretical works of hidden-charm pentaquarks before the LHCb announcement [4–7]. After the LHCb observation, many theoretical studies in various ways have been conducted: hadronic molecular picture [8–23], quark model estimation [24–26], diquark picture [27–31], quark-cluster model[32], baryocharmonium model[33], hadroquarkonia model[34], soliton model[35], holographic QCD [36], and hadronic molecule coupled with five-quark state [37]. Some review papers are also published [38–40].

The hadronic molecular picture is one of the highly possible model around the hadron threshold. The threshold of  $\bar{D}\Sigma_c^*$  is 4385.3 MeV and  $\bar{D}^*\Sigma_c$  is 4462.2 MeV. These values are slightly above the mass of  $P_c(4380)$  and  $P_c(4450)$ , respectively. Therefore, the  $P_c$  pentaquarks can be considered as the loosely bound states of a charmed meson and a charmed baryon.

In the heavy quark effective theory, the spin dependent interaction of heavy quark is suppressed by the inverse of the heavy quark mass,  $1/m_Q$ . At the heavy quark limit, therefore, the dynamics is independent of the trans-

formation of the heavy quark spin. This is called the heavy quark spin symmetry (HQSS). The suppression of the spin dependent force causes the decomposition of the heavy quark spin and the light-cloud spin at the heavy quark limit [41–45] :

$$\vec{J} = \vec{s}_{\text{light}} + \vec{s}_{\text{heavy}} . \quad (1)$$

The total angular momentum  $\vec{J}$  is a conserved quantity, and the heavy quark spin  $\vec{s}_{\text{heavy}}$  is conserved at heavy quark limit. Then, the light-cloud spin  $\vec{s}_{\text{light}}$  is also conserved.

The HQSS leads to the mass degeneracy between the heavy hadrons with different spin. Considering a heavy meson  $P^{(*)} \sim Q\bar{q}$  with a heavy quark  $Q$  and an anti-light quark  $\bar{q}$ , the total spin of  $Q\bar{q}$  is

$$J_{\pm} = 1/2 \pm 1/2 , \quad (2)$$

and  $J_+ = 1$  ( $J_- = 0$ ) for the vector meson  $P^*$  (the pseudoscalar meson  $P$ ), because of the quark spin  $1/2$ . Their difference comes from the spin configuration of the light cloud and heavy quark spins. However, the system is independent of the heavy quark spin and as a result, the spin 0 state  $P$  and the spin 1 state  $P^*$  degenerate at heavy quark limit. This structure is called the HQS doublet.

In the real world, however, the quark masses are finite, so that there exists a mass difference between the pseudoscalar and vector mesons. For example, the mass difference between pseudoscalar meson  $K$  and vector meson  $K^*$  is about 400 MeV. By contrast, the mass splitting between  $D$  and  $D^*$  is about 140MeV and between  $B$  and  $B^*$  is 45MeV. The mass difference is much smaller in the charm and bottom quark sectors than in the light quark sector. There is a same tendency in the single heavy baryon. The mass difference between spin  $1/2$  baryon  $\Sigma_c$  and spin  $3/2$  baryon  $\Sigma_c^*$  is about 65 MeV, and  $\Sigma_b$  and  $\Sigma_b^*$  is about 20 MeV. The HQSS approximately exists in the heavy quark sector.

\* yshimizu@hken.phys.nagoya-u.ac.jp

† yasuihiro.yamaguchi@riken.jp

‡ harada@hken.phys.nagoya-u.ac.jp

The purpose of this work is to study the HQS multiplet structure of  $Q\bar{Q}qqq$ -type pentaquarks as hadronic molecular states of a  $\bar{P}^{(*)}$  meson and a  $\Sigma_Q^{(*)}$  baryon. Here  $\bar{P}$  and  $\bar{P}^*$  denote mesons with  $J^P = 0^-$  and  $1^-$  with an anti-heavy quark like  $\bar{D}$  and  $\bar{D}^*$  mesons, and  $\Sigma_Q$  and  $\Sigma_Q^*$  the baryons with  $J^P = 1/2^+$  and  $3/2^+$  with a heavy quark like  $\Sigma_c$  and  $\Sigma_c^*$  baryons. We note that the HQS doublet structure of single heavy hadrons such as  $\bar{P}^{(*)}$  and  $\Sigma_Q^{(*)}$  is well known. Furthermore, the HQS multiplet structure of multi-hadron system with single heavy quark like  $\bar{P}^{(*)}N$  molecular states has been studied in Refs. [46–48]. On the other hand, the HQS multiplet structure of doubly heavy hadrons like  $Q\bar{Q}qqq$  pentaquarks is nontrivial. Hence, it is interesting to investigate the HQS multiplet structure of heavy meson-baryon molecular states.

In Ref. [49], the HQS multiplet structure of  $\bar{P}^{(*)}\Sigma_Q^{(*)}$  with S-wave has been studied. The analysis of the S-wave state covers the negative parity Pentaquarks. However, one of the  $P_c^+$  pentaquarks has the positive parity. Accordingly, we study possible positive parity states by considering P-wave molecular states of  $\bar{P}^{(*)}$  and  $\Sigma_Q^{(*)}$  in the present paper. We define the light-cloud spin (LCS) basis introduced in Ref. [49] which is useful to investigate the HQS multiplet structure. Although the hadronic molecular (HM) basis is simple to consider the possible total spin state and to construct the potentials, it is not useful to investigate the HQS multiplet structure because the heavy quark spin and the light-cloud spin are not separated in this basis. In the light-cloud spin (LCS) basis, however, these spins are separated explicitly as shown in Eq. (1). Below we shall transform the HM basis to the LCS basis and study the HQS multiplet structure. Moreover, we demonstrate which multiplets can be bound under the one-pion exchange potential (OPEP) from the heavy hadron effective theory.

This paper is organized as follows. In Sec. II we construct the HM basis of the  $\bar{P}^{(*)}\Sigma_Q^{(*)}$  states and transfer it to LCS basis to discuss the HQS multiplet structure. The OPEP is shown in Sec. III. In Sec. IV, we summarize the numerical results. Finally, Sec. V is a summary and discussion.

## II. HQS MULTIPLET STRUCTURE OF $\bar{P}^{(*)}\Sigma_Q^{(*)}$ WITH P-WAVE

In this section, we consider the HQS multiplet of P-wave states. First, we construct the hadronic molecular (HM) basis of the  $\bar{P}^{(*)}\Sigma_Q^{(*)}$  states. The possible spin states and meson-baryon components with given  $J^P$  are shown in Tab. I. Giving the  $\bar{P}^{(*)}\Sigma_Q^{(*)}$  component with total spin  $S$ , we obtain the spin structure in the HM basis and the possible total angular momentum  $J$  as follows:

$$\bar{P}\Sigma_Q(2P) = \left[ P \left[ [\bar{Q}q]_0 [Q[d]_{11/2}]_{1/2} \right] \right] = \frac{1}{2} \oplus \frac{3}{2}, \quad (3)$$

$$\bar{P}\Sigma_Q^*(4P) = \left[ P \left[ [\bar{Q}q]_0 [Q[d]_{13/2}]_{3/2} \right] \right] = \frac{1}{2} \oplus \frac{3}{2} \oplus \frac{5}{2}, \quad (4)$$

$$\bar{P}^*\Sigma_Q(2P) = \left[ P \left[ [\bar{Q}q]_1 [Q[d]_{11/2}]_{1/2} \right] \right] = \frac{1}{2} \oplus \frac{3}{2}, \quad (5)$$

$$\bar{P}^*\Sigma_Q(4P) = \left[ P \left[ [\bar{Q}q]_1 [Q[d]_{11/2}]_{3/2} \right] \right] = \frac{1}{2} \oplus \frac{3}{2} \oplus \frac{5}{2}, \quad (6)$$

$$\bar{P}^*\Sigma_Q^*(2P) = \left[ P \left[ [\bar{Q}q]_1 [Q[d]_{13/2}]_{1/2} \right] \right] = \frac{1}{2} \oplus \frac{3}{2}, \quad (7)$$

$$\bar{P}^*\Sigma_Q^*(4P) = \left[ P \left[ [\bar{Q}q]_1 [Q[d]_{13/2}]_{3/2} \right] \right] = \frac{1}{2} \oplus \frac{3}{2} \oplus \frac{5}{2}, \quad (8)$$

$$\bar{P}^*\Sigma_Q^*(6P) = \left[ P \left[ [\bar{Q}q]_1 [Q[d]_{13/2}]_{5/2} \right] \right] = \frac{3}{2} \oplus \frac{5}{2} \oplus \frac{7}{2}, \quad (9)$$

where  $\left[ L \left[ [\bar{Q}q]_{s_1} [Q[d]_{1s_2}]_S \right] \right]$  implies that the  $\bar{P}^{(*)} \sim \bar{Q}q$  meson with spin  $s_1$  and the  $\Sigma_Q^{(*)} \sim Qd$  baryon ( $d = qq$  is a light diquark) with spin  $s_2$  are combined into a  $\bar{P}^{(*)}\Sigma_Q^{(*)}$  composite state with the total spin  $S$  and the orbital angular momentum  $L$ .  $[d]_1$  implies that the spin of the diquark is 1. HM basis is simple to construct the possible spin states because it is just the coupling of the spins of the meson and baryon and the orbital angular momentum. However, HM basis is not suitable to discuss the HQS multiplet structure. The heavy quark spin and the light-cloud spin are independently conserved in the heavy quark limit. Thereby, the heavy quark spin and the other spin must be treated separately. We define the light-cloud spin (LCS) basis as a suitable basis to study the structure of HQS multiplets.

In the LCS basis, the spin structures are rewritten as follows :

$$(s-1) : \left[ [\bar{Q}Q]_0 \left[ P [q [d]_{11/2}]_{1/2} \right] \right] = \frac{1}{2}, \quad (10)$$

$$(s-2) : \left[ [\bar{Q}Q]_0 \left[ P [q [d]_{13/2}]_{1/2} \right] \right] = \frac{1}{2}, \quad (11)$$

$$(s-3) : \left[ [\bar{Q}Q]_0 \left[ P [q [d]_{11/2}]_{3/2} \right] \right] = \frac{3}{2}, \quad (12)$$

$$(s-4) : \left[ [\bar{Q}Q]_0 \left[ P [q [d]_{13/2}]_{3/2} \right] \right] = \frac{3}{2}, \quad (13)$$

$$(s-5) : \left[ [\bar{Q}Q]_0 \left[ P [q [d]_{13/2}]_{5/2} \right] \right] = \frac{5}{2}, \quad (14)$$

$$(d-1) : \left[ [\bar{Q}Q]_1 \left[ P [q [d]_{11/2}]_{1/2} \right] \right] = \frac{1}{2} \oplus \frac{3}{2}, \quad (15)$$

$$(d-2) : \left[ [\bar{Q}Q]_1 \left[ P [q [d]_{13/2}]_{1/2} \right] \right] = \frac{1}{2} \oplus \frac{3}{2}, \quad (16)$$

$$(t-1) : \left[ [\bar{Q}Q]_1 \left[ P [q [d]_{11/2}]_{3/2} \right] \right] = \frac{1}{2} \oplus \frac{3}{2} \oplus \frac{5}{2}, \quad (17)$$

TABLE I. Possible spin states of the P-wave  $\bar{P}^{(*)}\Sigma_Q^{(*)}$  molecular states with given  $J^P$ . ( $^{2S+1}L_J$ ) denotes the total spin of meson and baryon  $S$ , the orbital angular momentum  $L$ , and the total angular momentum  $J$ .

$J^P$	
$\frac{1}{2}^+$	$\bar{P}\Sigma_Q(^2P_{1/2}), \bar{P}\Sigma_Q^*(^4P_{1/2}), \bar{P}^*\Sigma_Q(^2P_{1/2}), \bar{P}^*\Sigma_Q(^4P_{1/2}), \bar{P}^*\Sigma_Q^*(^2P_{1/2}), \bar{P}^*\Sigma_Q^*(^4P_{1/2})$
$\frac{3}{2}^+$	$\bar{P}\Sigma_Q(^2P_{3/2}), \bar{P}\Sigma_Q^*(^4P_{3/2}), \bar{P}^*\Sigma_Q(^2P_{3/2}), \bar{P}^*\Sigma_Q(^4P_{3/2}), \bar{P}^*\Sigma_Q^*(^2P_{3/2}), \bar{P}^*\Sigma_Q^*(^4P_{3/2}), \bar{P}^*\Sigma_Q^*(^6P_{3/2})$
$\frac{5}{2}^+$	$\bar{P}\Sigma_Q^*(^4P_{5/2}), \bar{P}^*\Sigma_Q(^4P_{5/2}), \bar{P}^*\Sigma_Q^*(^4P_{5/2}), \bar{P}^*\Sigma_Q^*(^6P_{5/2})$
$\frac{7}{2}^+$	$\bar{P}^*\Sigma_Q^*(^6P_{7/2})$

$$(t-2) : \left[ [\bar{Q}Q]_1 \left[ P[q[d]_{13/2}]_{3/2} \right] \right] = \frac{1}{2} \oplus \frac{3}{2} \oplus \frac{5}{2}, \quad (18)$$

$$(t-3) : \left[ [\bar{Q}Q]_1 \left[ P[q[d]_{13/2}]_{5/2} \right] \right] = \frac{3}{2} \oplus \frac{5}{2} \oplus \frac{7}{2}, \quad (19)$$

where  $[\bar{Q}Q]_{s_1} \left[ P[q[d]_{1s_2}]_{s_3} \right]$  implies the followings: A heavy quark  $Q$  and an anti-heavy quark  $\bar{Q}$  are combined into a state with spin  $s_1$  in S-wave. Spins of a light quark  $q$  and a diquark  $d$  are coupled to spin  $s_2$  and the total spin of the combined state in P-wave is given by  $s_3$ . The right hand side of the equation shows the possible spins of the combined pentaquark states. There exist five HQS singlets (s-1 to s-5), two HQS doublets (d-1 and d-2), and three HQS triplets (t-1 to t-3). The HQS triplet does not exist in single heavy hadrons. It is a feature of the multi-heavy quark system. The basis transformation is done by

$$\psi_{JP}^{\text{LCS}} = U_{JP}^{-1} \psi_{JP}^{\text{HM}}, \quad (20)$$

where the  $U$  is a transformation matrix determined by the Clebsch-Gordan coefficient to reconstruct the spin structure. The detail of the basis transformation is summarized in Appendix A. It is to be noted that the two heavy quarks are labeled by the same velocity  $v$  to classify the pentaquark states based on the heavy quark spin symmetry.

### III. POTENTIALS

In the previous section, we showed that there are ten multiplets in the P-wave  $\bar{P}^{(*)}\Sigma_Q^{(*)}$  molecular states. In this section, we demonstrate that which of the multiplets can be bound by using one-pion exchange potential (OPEP). We construct the OPEP for  $\bar{P}^{(*)}\Sigma_Q^{(*)}$  molecular states based on the heavy hadron effective theory.

The  $\bar{P}^{(*)}$  meson and pion interaction Lagrangian is given in Refs.[50–54], and the  $\Sigma_Q^{(*)}$  baryon and pion interaction Lagrangian is given in Refs.[53, 55]. See also our previous paper [49].

When we construct the OPEP from effective Lagrangians, we introduce a cutoff parameter  $\Lambda$  via the monopole type form factor

$$F(q) = \frac{\Lambda^2 - m_\pi^2}{\Lambda^2 + |\vec{q}|^2}, \quad (21)$$

at each vertex, where  $m_\pi$  is the mass of the exchanging pion, and  $\vec{q}$  is its momentum. We use the same cutoff for  $\bar{P}^{(*)}\bar{P}^{(*)}\pi$  and  $\Sigma_Q^{(*)}\Sigma_Q^{(*)}\pi$  vertices for simplicity, and fix the value of cutoff 1000 MeV and 1500 MeV. The obtained potential matrices in the HM basis are summarized in Appendix A. We note that contact terms are subtracted from the potentials, because in a conventional way, the OPEP has been considered at large distance [56]. Furthermore, we study the cases where the final pentaquarks carry isospin 1/2, because  $P_c$  pentaquarks carry  $I = 1/2$ .

The potential matrices can be also transformed to LCS basis by using the unitary matrix  $U$  as follows:

$$V_{1/2^+}^{\text{LCS}} = U_{1/2^+}^{-1} V_{1/2^+}^{\text{HM}} U_{1/2^+} = \begin{pmatrix} C & -\frac{\sqrt{2}}{2}T & 0 & 0 & 0 & 0 \\ -\frac{\sqrt{2}}{2}T & -\frac{1}{2}C + T & 0 & 0 & 0 & 0 \\ 0 & 0 & C & -\frac{\sqrt{2}}{2}T & 0 & 0 \\ 0 & 0 & -\frac{\sqrt{2}}{2}T & -\frac{1}{2}C + T & 0 & 0 \\ 0 & 0 & 0 & 0 & C & \frac{\sqrt{5}}{10}T \\ 0 & 0 & 0 & 0 & \frac{\sqrt{5}}{10}T & -\frac{1}{2}C - \frac{4}{5}T \end{pmatrix} \frac{gg_1}{f_\pi^2}, \quad (22)$$

$$\begin{aligned}
V_{3/2^+}^{\text{LCS}} &= U_{3/2^+}^{-1} V_{3/2^+}^{\text{HM}} U_{3/2^+} \\
&= \begin{pmatrix} C & \frac{\sqrt{5}}{10}T & 0 & 0 & 0 & 0 & 0 \\ \frac{\sqrt{5}}{10}T & -\frac{1}{2}C - \frac{4}{5}T & 0 & 0 & 0 & 0 & 0 \\ 0 & 0 & C & -\frac{\sqrt{2}}{2}T & 0 & 0 & 0 \\ 0 & 0 & -\frac{\sqrt{2}}{2}T & -\frac{1}{2}C + T & 0 & 0 & 0 \\ 0 & 0 & 0 & 0 & C & \frac{\sqrt{5}}{10}T & 0 \\ 0 & 0 & 0 & 0 & \frac{\sqrt{5}}{10}T & -\frac{1}{2}C - \frac{4}{5}T & 0 \\ 0 & 0 & 0 & 0 & 0 & 0 & -\frac{1}{2}C + \frac{1}{5}T \end{pmatrix} \frac{gg_1}{f_\pi^2}, \quad (23)
\end{aligned}$$

$$\begin{aligned}
V_{5/2^+}^{\text{LCS}} &= U_{5/2^+}^{-1} V_{5/2^+}^{\text{HM}} U_{5/2^+} \\
&= \begin{pmatrix} -\frac{1}{2}C + \frac{1}{5}T & 0 & 0 & 0 \\ 0 & C & \frac{\sqrt{5}}{10}T & 0 \\ 0 & \frac{\sqrt{5}}{10}T & -\frac{1}{2}C - \frac{4}{5}T & 0 \\ 0 & 0 & 0 & -\frac{1}{2}C + \frac{1}{5}T \end{pmatrix} \frac{gg_1}{f_\pi^2}, \quad (24)
\end{aligned}$$

$$\begin{aligned}
V_{7/2^+}^{\text{LCS}} &= U_{7/2^+}^{-1} V_{7/2^+}^{\text{HM}} U_{7/2^+} \\
&= \frac{gg_1}{f_\pi^2} \left[ -\frac{1}{2}C + \frac{1}{5}T \right], \quad (25)
\end{aligned}$$

where the functions  $C(m_\pi, r, \Lambda)$  and  $T(m_\pi, r, \Lambda)$  are the spin-spin potential and tensor potential, respectively. We omitted the arguments of potentials in the above equations. Their explicit forms are given by

$$C(m_\pi, r, \Lambda) = \frac{m_\pi^2}{4\pi} \left[ \frac{e^{-m_\pi r} - e^{-\Lambda r}}{r} - \frac{\Lambda^2 - m_\pi^2}{2\Lambda} e^{-\Lambda r} \right], \quad (26)$$

$$T(m_\pi, r, \Lambda) = \frac{m_\pi^3}{4\pi} H_3(m_\pi, \Lambda, r), \quad (27)$$

$$\begin{aligned}
H_3(m_\pi, \Lambda, r) &= \frac{1}{m_\pi^3} \left[ \frac{m_\pi^2 r^2 + 3m_\pi r + 3}{r^3} e^{-m_\pi r} \right. \\
&\quad - \frac{\Lambda^2 r^2 + 3\Lambda r + 3}{r^3} e^{-\Lambda r} \\
&\quad \left. - \frac{\Lambda^2 - m_\pi^2}{2r} e^{-\Lambda r} - \frac{\Lambda^3 - \Lambda m_\pi^2}{2} e^{-\Lambda r} \right]. \quad (28)
\end{aligned}$$

The typical shapes of  $C$  and  $T$  are shown in Fig.1. This shows that the signs  $C$  and  $T$  are negative so as to be attractive potentials. The heavy meson - pion coupling constant  $|g| = 0.59$  is determined by the decay of  $D^* \rightarrow D\pi$  [57], the heavy baryon - pion coupling constant  $g_1 = 0.94$  is estimated by the quark model in Ref.[55], and the pion decay constant is  $f_\pi = 92.4$  MeV.

The block matrices of the above OPEPs in LCS basis are classified by the HQS multiplet structure. For example, the first  $2 \times 2$  block in Eq.(22) is for HQS singlet sector with the total spin  $1/2$ . It corresponds to the first and second component in Eq.(A6), or (s-1) component in Eq.(10) and (s-2) in Eq.(11). Similarly, the second block in Eq.(22) corresponds to the third and fourth component

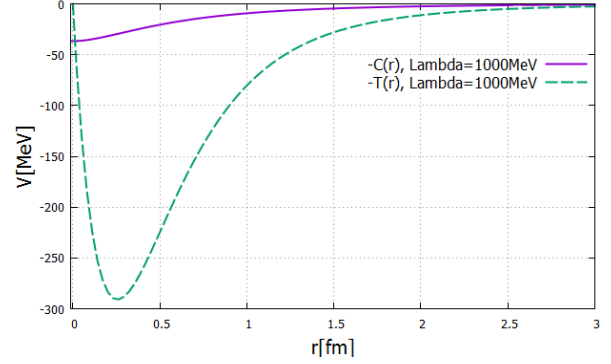


FIG. 1. Spin-spin potential  $C$  and tensor potential  $T$  with the cutoff parameter  $\Lambda = 1000$  MeV.

in Eq.(A6) which is for spin  $(1/2, 3/2)$  doublet, and the third block in Eq.(22) corresponds to the fifth and sixth component in Eq.(A6) which is for spin  $(1/2, 3/2, 5/2)$  triplet.

The component of block matrix is determined by the structure of the light-cloud spin. For instance, the first and second block in Eq.(22) are identical because two  $1/2$  singlets and two  $(1/2, 3/2)$  doublets have the same light-cloud spin structure,  $\left[ P[q[d]_1]_{1/2} \right]_{1/2}$  and  $\left[ P[q[d]_1]_{3/2} \right]_{1/2}$ , as shown in Eq.(A6).

#### IV. NUMERICAL RESULT

In this section we show the binding energy obtained by solving the coupled channel Schrödinger equation under the OPEPs obtained in the previous section. We use the Gaussian expansion method [58] to solve the Schrödinger

TABLE II. Masses of relevant charmed and bottomed hadrons [57].

	$\bar{D}$	$\bar{D}^*$	$B$	$B^*$
Mass[MeV]	1867.21	2008.56	5279.48	5324.65
	$\Sigma_c$	$\Sigma_c^*$	$\Sigma_b$	$\Sigma_b^*$
Mass[MeV]	2453.54	2518.13	5813.4	5833.6

equations. As discussed in Ref.[49], the coupling constant has a sign ambiguity. This ambiguity is the relative sign between the heavy meson - pion coupling  $g$  and the heavy baryon - pion coupling  $g_1$ . We assign the same sign as the quark model estimation in Ref.[55] as the sign of  $g_1$ . Therefore, we treat the sign uncertainty as the sign of  $g$ . In this study, we investigate both cases.

We include the effect of the heavy quark spin symmetry breaking by introducing the mass difference between two heavy mesons (baryons) in one HQS doublet, namely  $\bar{P}$  and  $\bar{P}^*$  ( $\Sigma_Q$  and  $\Sigma_Q^*$ ). We parameterize the heavy hadron masses as done in Ref.[49] :

$$M_{\bar{P}} = 2\mu + \frac{a}{2\mu} + \frac{w}{(2\mu)^2}, \quad (29)$$

$$M_{\bar{P}^*} = 2\mu + \frac{b}{2\mu} + \frac{x}{(2\mu)^2}, \quad (30)$$

$$M_{\Sigma_Q} = 2\mu + \frac{c}{2\mu} + \frac{y}{(2\mu)^2}, \quad (31)$$

$$M_{\Sigma_Q^*} = 2\mu + \frac{d}{2\mu} + \frac{z}{(2\mu)^2}. \quad (32)$$

The mass parameter  $\mu$  controls the typical mass scale. It corresponds to the averaged reduced mass of  $\bar{P}\Sigma_Q$ ,  $\bar{P}\Sigma_Q^*$ ,  $\bar{P}^*\Sigma_Q$ , and  $\bar{P}^*\Sigma_Q^*$ . We determine the eight parameters  $a, b, c, d, w, x, y$ , and  $z$  to reproduce the eight hadron masses shown in Table II. The value of eight parameters are summarized in Table III. When  $\mu = 1.102$  and  $2.779$  GeV, the charmed and the bottomed hadron masses are reproduced, respectively. The heavy quark spin symmetry restores as the mass parameter  $\mu$  increases.

Firstly, we show the numerical results obtained by solving the coupled channel Schrödinger equations for each structure of light-cloud spin in the case of  $g = +0.59$ . In this case, the multiplets which have the light-clouds  $\left[ P [q [d]_1]_{1/2} \right]_{1/2}$  and  $\left[ P [q [d]_1]_{3/2} \right]_{3/2}$  are attractive. In Fig.2, we show the energy of  $\left[ P [q [d]_1]_{1/2} \right]_{1/2}$ , which corresponds to the spin 1/2 singlet (s-1) in Eq. (10) and spin (1/2, 3/2) doublet (d-1) in Eq. (15). The labels in Fig. 2 to Fig. 6 are named by a main component of the wave function at the heavy quark limit. Here, all the energies for three states are measured from the lowest threshold of  $\bar{P}\Sigma_Q$ . Their energies are almost degenerate at whole range of  $\mu$ . Next, in Fig. 3, we show the energy of  $\left[ P [q [d]_1]_{3/2} \right]_{3/2}$ , which corresponds to the spin 3/2 singlet (s-4) in Eq. (13) and spin (1/2, 3/2, 5/2) triplet

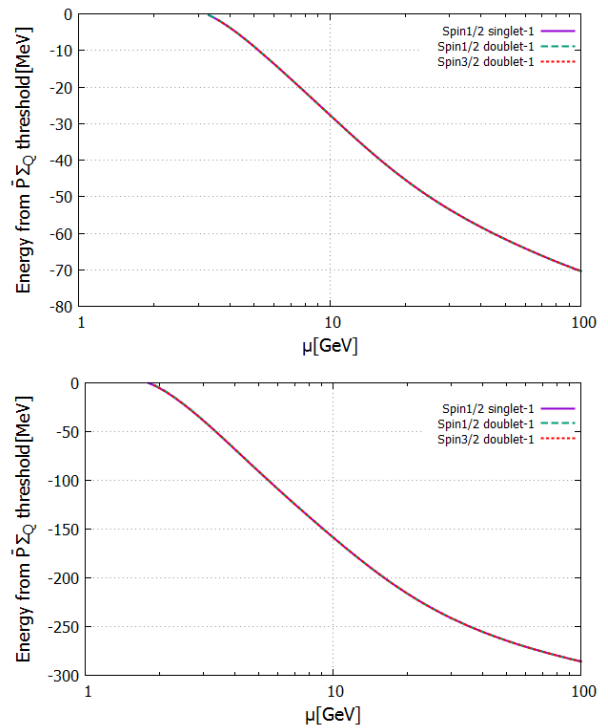


FIG. 2. Energies for singlet-1 and doublet-1 which have the light-cloud spin structure of  $\left[ P [q [d]_1]_{1/2} \right]_{1/2}$  with  $g = +0.59$ . The cutoff parameter is  $\Lambda = 1000$  MeV (upper figure) and  $\Lambda = 1500$  MeV (lower figure). The energy is measured from the threshold of  $\bar{P}\Sigma_Q$ . Reduced mass parameter is changed from 1 GeV to 100 GeV. The labels are defined by the main component at heavy quark limit.

(t-2) in Eq. (18). We note that the lowest threshold of the spin 1/2 and 3/2 states is  $\bar{P}\Sigma_Q$ , while that of the spin 5/2 state is  $\bar{P}\Sigma_Q^*$ . Then, the energies of spin-5/2 state shown in Fig. 3 (and Figs. 4 and 6) are positive even if they are bound states. For example, in the result of  $\Lambda = 1000$  MeV, the mass of spin 5/2 state is 4381.6 MeV at  $\mu = 1.102$  GeV. This value is very close to the mass of  $P_c^+$  (4380).

Next, we show the result of  $g = -0.59$ . The multiplets with  $\left[ P [q [d]_1]_{1/2} \right]_{3/2}$ ,  $\left[ P [q [d]_1]_{3/2} \right]_{1/2}$ , and  $\left[ P [q [d]_1]_{3/2} \right]_{5/2}$  are attractive. We show the energy of  $\left[ P [q [d]_1]_{1/2} \right]_{3/2}$  in Fig. 4, which corresponds to the spin 3/2 singlet (s-3) in Eq.(12) and spin (1/2, 3/2, 5/2) triplet (t-1) in Eq.(17). The lowest threshold of the spin 1/2 and 3/2 states is  $\bar{P}\Sigma_Q$ , while the spin 5/2 state is  $\bar{P}\Sigma_Q^*$ . Next, the energy of  $\left[ P [q [d]_1]_{3/2} \right]_{1/2}$  is shown in Fig. 5, which corresponds to the spin 1/2 singlet (s-2) in Eq.(11) and spin (1/2, 3/2) doublet (d-2) in Eq.(16). Finally, we show the energy of  $\left[ P [q [d]_1]_{3/2} \right]_{5/2}$  in Fig. 6,

TABLE III. Values of parameters to include the effect of heavy quark spin symmetry breaking in Eqs.(29)-(32).

$a[\text{GeV}^2]$	$b[\text{GeV}^2]$	$c[\text{GeV}^2]$	$d[\text{GeV}^2]$	$w[\text{GeV}^3]$	$x[\text{GeV}^3]$	$y[\text{GeV}^3]$	$z[\text{GeV}^3]$
-2.0798	-1.8685	1.9889	2.0814	2.9468	3.1677	-3.1729	-3.0629

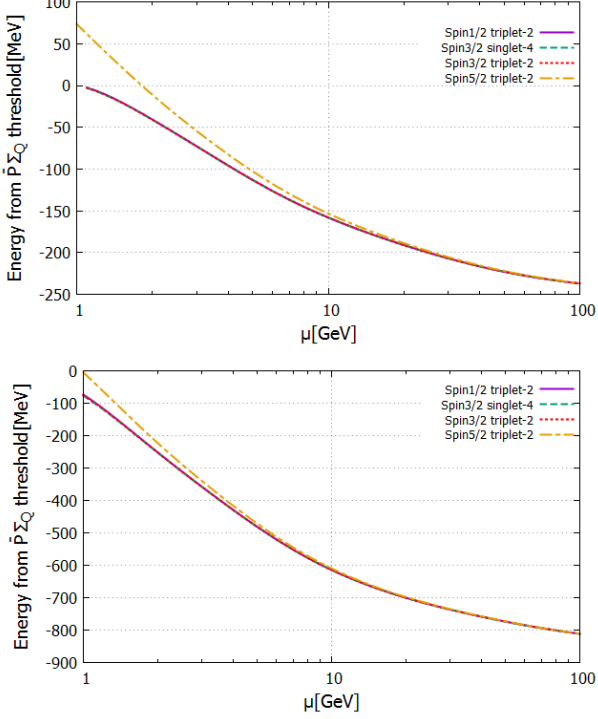


FIG. 3. Energies for singlet-4 and triplet-2 which have the light-cloud spin structure of  $\left[ P \left[ q \left[ d_1 \right]_{3/2} \right]_{3/2} \right]$  with  $g = +0.59$ . The cutoff parameter is  $\Lambda = 1000$  MeV (upper figure) and  $\Lambda = 1500$  MeV (lower figure) .

which corresponds to the spin 5/2 singlet (s-5) in Eq.(14) and spin (3/2, 5/2, 7/2) triplet (t-3) in Eq.(19). We note that the threshold of the spin 7/2 state is measured from  $\bar{P}^* \Sigma_Q^*$ . The difference of threshold values between  $\bar{P} \Sigma_Q$  and  $\bar{P} \Sigma_Q^*$  is 73.774 MeV, and between  $\bar{P} \Sigma_Q$  and  $\bar{P}^* \Sigma_Q^*$  is 234.63 MeV at  $\mu = 1.0$  GeV.

The states which have same structure of light-cloud spin are degenerate at heavy quark limit. However, the heavy quark spin symmetry is broken for finite quark mass, and the mass degeneracy is resolved. We summarize the values of the masses of obtained bound states at the charm region ( $\mu = 1.102$  GeV) and bottom region ( $\mu = 2.779$  GeV) in Table IV-VII. For instance, in Table. IV, the mass difference between  $J^P = 3/2^+$  and  $5/2^+$  in HQS triplet-3 is 64.2 MeV at  $\mu = 1.102$  GeV, and 24 MeV at  $\mu = 2.779$  GeV. This shows that the mass difference becomes smaller in the bottom sector. Although the present study includes only OPEP, the mass degen-

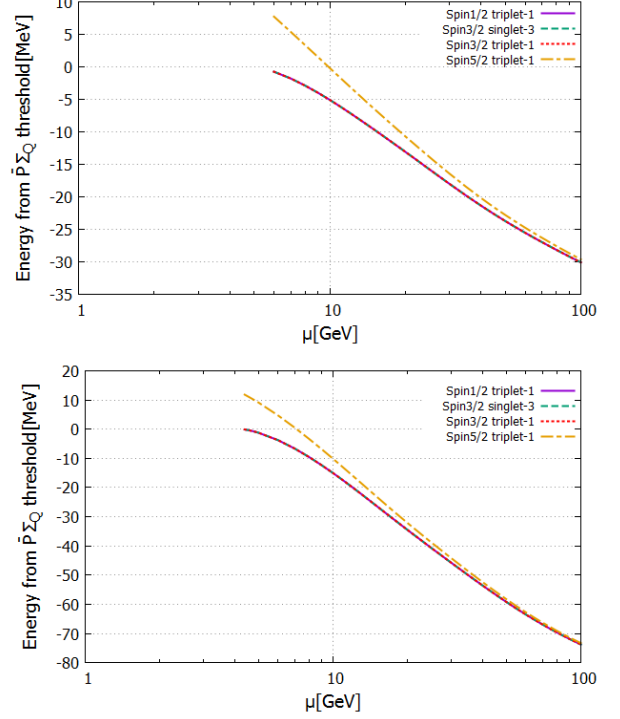


FIG. 4. Energies for singlet-3 and triplet-1 which have the light-cloud spin structure of  $\left[ P \left[ q \left[ d_1 \right]_{1/2} \right]_{3/2} \right]$  with  $g = -0.59$ . The cutoff parameter is  $\Lambda = 1000$  MeV (upper figure) and  $\Lambda = 1500$  MeV (lower figure) .

eracy should occur even using the more realistic potential model if the heavy quark spin symmetry exists in the doubly heavy hadronic molecule. The search for the HQS partner states of  $P_c$ -like pentaquark is very important to understand the structure of heavy hadrons.

## V. SUMMARY AND DISCUSSIONS

In Sec.II, we showed the HQS multiplet structure of molecular states made from a heavy meson and a heavy baryon in P-wave. There are five HQS singlets, two doublets, and three triplets. The potential matrix is block diagonalized in the LCS basis for each HQS multiplet as shown in Sec. III. We obtained the binding energy by solving the Schrödinger equation under OPEP in Sec. IV. When  $g$  is positive, the spin 1/2 singlet (s-1), 3/2 singlet (s-4), the blocks of the potential for (1/2, 3/2) dou-

TABLE IV. Masses of bound states in unit of MeV with  $\Lambda = 1000$  MeV and  $g = +0.59$  at  $\mu = 1.102$  and  $2.779$  GeV.

$\mu$ [GeV]	Spin 1/2			Spin 3/2			Spin 5/2
	singlet-1	doublet-1	triplet-2	singlet-4	doublet-1	triplet-2	triplet-2
1.102	no bound	no bound	4317.7	4317.1	no bound	4317.4	4381.6
2.779	no bound	no bound	11025	11025	no bound	11025	11049

TABLE V. Masses of bound states in unit of MeV with  $\Lambda = 1500$  MeV and  $g = +0.59$  at  $\mu = 1.102$  and  $2.779$  GeV.

$\mu$ [GeV]	Spin 1/2			Spin 3/2			Spin 5/2
	singlet-1	doublet-1	triplet-2	singlet-4	doublet-1	triplet-2	triplet-2
1.102	no bound	no bound	4225.4	4222.3	no bound	4223.7	4285.3
2.779	11060	11060	10752	10752	11060	10752	11060

TABLE VI. Masses of bound states in unit of MeV with  $\Lambda = 1000$  MeV and  $g = -0.59$  at  $\mu = 1.102$  and  $2.779$  GeV.

$\mu$ [GeV]	Spin 1/2			Spin 3/2			
	singlet-2	doublet-2	triplet-1	singlet-3	doublet-2	triplet-1	triplet-3
1.102	4279.7	4281.0	no bound	no bound	4280.0	no bound	no bound
2.779	10947	10947	no bound	no bound	10942	no bound	no bound
$\mu$ [GeV]	Spin 5/2			Spin 7/2			
	singlet-5	triplet-1	triplet-3	triplet-3			
1.102	no bound	no bound	no bound	no bound			
2.779	no bound	no bound	no bound	no bound			

TABLE VII. Masses of bound states in unit of MeV with  $\Lambda = 1500$  MeV and  $g = -0.59$  at  $\mu = 1.102$  and  $2.779$  GeV.

$\mu$ [GeV]	Spin 1/2			Spin 3/2			
	singlet-2	doublet-2	triplet-1	singlet-3	doublet-2	triplet-1	triplet-3
1.102	3993.9	3998.7	no bound	no bound	3994.9	no bound	no bound
2.779	10401	10401	no bound	no bound	10401	no bound	no bound
$\mu$ [GeV]	Spin 5/2			Spin 7/2			
	singlet-5	triplet-1	triplet-3	triplet-3			
1.102	no bound	no bound	no bound	no bound			
2.779	no bound	no bound	no bound	no bound			

plet (d-1), and  $(1/2, 3/2, 5/2)$  triplet (t-2) are attractive. The blocks for other six multiplets,  $1/2$  singlet (s-2),  $3/2$  singlet (s-3),  $5/2$  singlet (s-5),  $(1/2, 3/2)$  doublet (d-2),  $(1/2, 3/2, 5/2)$  triplet (t-1), and  $(3/2, 5/2, 7/2)$  triplet (t-3) are attractive when  $g$  is negative. The behavior of the binding energy is classified by the structure of the light-cloud spin. As mentioned in Ref.[49], OPEP depends only on the structure of the light-cloud spin since the pion exchange interaction couples the light quark spin and the orbital angular momentum. The HQS multiplets having the same light-cloud structure are degenerate at heavy quark limit. The mass degeneracy is resolved for hidden-charm/bottom pentaquarks because of the finite quark mass.

The mass of the  $J^P = 5/2^+$  state in Tab. IV is close to

the one of  $P_c^+(4380)$ . It's HQS triplet partner states carrying  $J^P = 1/2^+$  and  $3/2^+$  exist around 4320 MeV. The masses of their hidden-bottom flavor partner are 11025 MeV for  $J^P = 1/2^+$  and  $3/2^+$  states, and 11049 MeV for  $5/2^+$  states. We expect that these partner states will be found in future experiments.

When  $P_c^+(4380)$  is  $J^P = 5/2^+$ ,  $P_c^+(4450)$  should be  $3/2^-$ . We did not obtain such state in our previous work [49], since the mass of  $P_c^+(4450)$  is above the threshold of our coupled channel. The full coupled channel analysis of  $\bar{D}^{(*)}\Lambda_c - \bar{D}^{(*)}\Sigma_c^{(*)}$  using the complex scaling method was done in Ref.[19], which shows that it seems to be difficult to explain the mass and decay width of both  $P_c(4380)$  and  $P_c(4450)$  at the same time. Moreover,  $P_c$  pentaquarks are not reproduced by the estimation of compact five-body

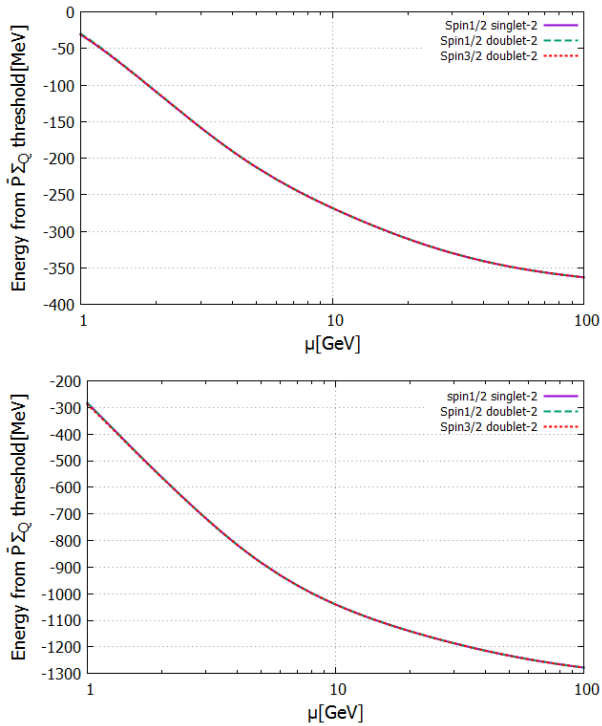


FIG. 5. Energies for singlet-2 and doublet-2 which have the light-cloud spin structure of  $\left[ P [q [d]_1 ]_{3/2} \right]_{1/2}$  with  $g = -0.59$ . The cutoff parameter is  $\Lambda = 1000$  MeV (upper figure) and  $\Lambda = 1500$  MeV (lower figure) .

pentaquark [26]. Some works argue that it is a threshold cusp by kinematical effect [59–62]. More theoretical efforts and experimental data are needed to reveal the nature of the  $P_c$  pentaquarks.

We determined the names of the solutions by the dominant component of the wave function, which we obtain together with the binding energy when solving the Schrödinger equation. For instance, in Fig.7 and Fig.8, we show the obtained wave functions of singlet-1 and triplet-2 with  $J^P = 1/2^+$ , for which the binding energies are shown in Fig.2 and Fig.3, respectively. We note that these wave functions are not normalized, therefore only the ratio of components is meaningful. In both cases, the change in the ratio of the wave functions when changing the mass parameter is very small. In the case of the finite quark mass, although the different components of the HQS multiplet are mixed, the ratio is still small. This shows that the effect of the symmetry breaking by the kinetic terms is small. When the mass parameter becomes larger, the wave functions concentrate at a position where the tensor potential becomes deep. This means that as the mass increases, the kinetic term is suppressed and the wave function is localized at the bottom of the attractive potential.

To treat the heavy quark spin symmetry for doubly heavy system, we assume that two heavy quarks in a pen-

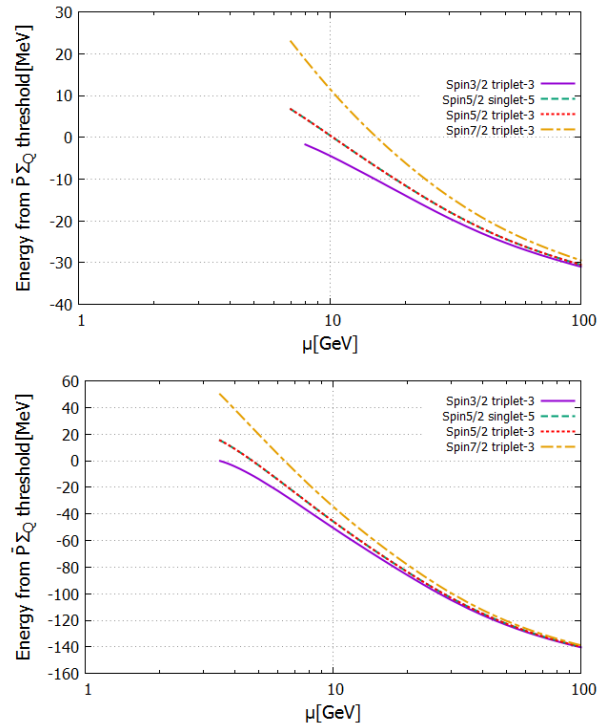


FIG. 6. Energies for singlet-5 and triplet-3 which have the light-cloud spin structure of  $\left[ P [q [d]_1 ]_{3/2} \right]_{5/2}$  with  $g = -0.59$ . The cutoff parameter is  $\Lambda = 1000$  MeV (upper figure) and  $\Lambda = 1500$  MeV (lower figure) .

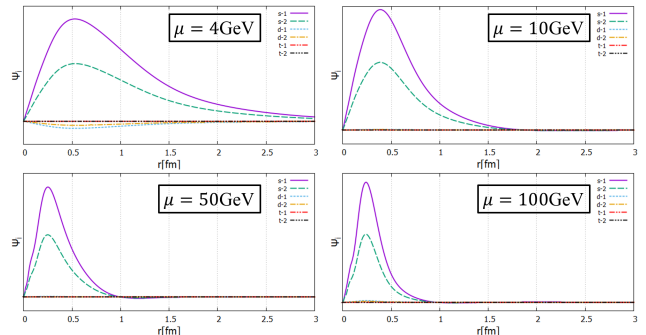


FIG. 7. Wave functions of singlet-1 state with  $J^P = 1/2^+$ ,  $g = +0.59$  and  $\Lambda = 1000$  MeV. The case of four different mass parameters are shown.

taquark are labeled by the same velocity. This assumption seems to be natural to the bound state because a hadronic molecule breaks when the relative velocity between the meson and baryon is large. However, if the heavy meson and heavy baryon are labeled by the same velocity, they can not get the orbital angular momentum excitation. To include the P-wave excitation we label one hadron by  $v$  and another by  $v'$ , and assume that their dif-



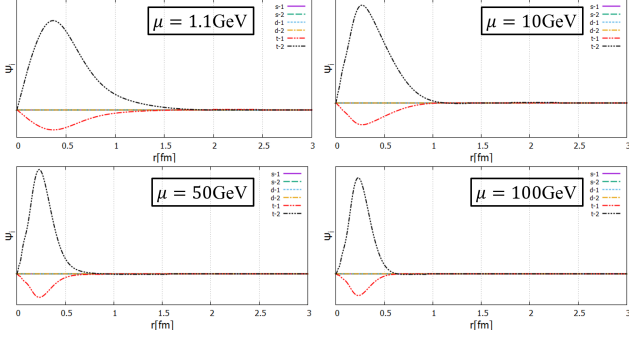


FIG. 8. Wave functions of triplet-2 state with  $J^P = 1/2^+$ ,  $g = +0.59$  and  $\Lambda = 1000$  MeV. The case of four different mass parameters are shown.

ference is small. Namely, when  $v'$  is written as  $v' = v + \delta v$  with the small quantity  $\delta v$ , we classify the HQS multiplet structure of P-wave states at the leading order of  $v'$  by neglecting  $\delta v$ . We do not include the effect of  $\delta v$  in the present study and leave the inclusion of its effects for future publications.

## ACKNOWLEDGMENTS

The work of Y.S. is supported in part by JSPS Grant-in-Aid for JSPS Research Fellow No. JP17J06300. The work of Y.Y. is supported in part by the Special Postdoctoral Researcher (SPDR) and iTHEMS Programs of RIKEN. The work of M.H. is supported in part by JPSP KAKENHI Grant Number 16K05345.

## Appendix A: Basis transformation

We show the detail of the transformation from HM basis to LCS basis. The wave function transformation is done by Eq.(20). The component of wave functions in HM basis for each spin state is

$$\psi_{1/2^+}^{\text{HM}} = \begin{pmatrix} \bar{P}\Sigma_Q(^2P_{1/2}) \\ \bar{P}\Sigma_Q^*(^4P_{1/2}) \\ \bar{P}^*\Sigma_Q(^2P_{1/2}) \\ \bar{P}^*\Sigma_Q(^4P_{1/2}) \\ \bar{P}^*\Sigma_Q^*(^2P_{1/2}) \\ \bar{P}^*\Sigma_Q^*(^4P_{1/2}) \end{pmatrix}, \quad (\text{A1})$$

$$\psi_{3/2^+}^{\text{HM}} = \begin{pmatrix} \bar{P}\Sigma_Q(^2P_{3/2}) \\ \bar{P}\Sigma_Q^*(^4P_{3/2}) \\ \bar{P}^*\Sigma_Q(^2P_{3/2}) \\ \bar{P}^*\Sigma_Q(^4P_{3/2}) \\ \bar{P}^*\Sigma_Q^*(^2P_{3/2}) \\ \bar{P}^*\Sigma_Q^*(^4P_{3/2}) \\ \bar{P}^*\Sigma_Q^*(^6P_{3/2}) \end{pmatrix}, \quad (\text{A2})$$

$$\psi_{5/2^+}^{\text{HM}} = \begin{pmatrix} \bar{P}\Sigma_Q^*(^4P_{5/2}) \\ \bar{P}^*\Sigma_Q(^4P_{5/2}) \\ \bar{P}^*\Sigma_Q^*(^4P_{5/2}) \\ \bar{P}^*\Sigma_Q^*(^6P_{5/2}) \end{pmatrix}, \quad (\text{A3})$$

$$\psi_{7/2^+}^{\text{HM}} = \left( \bar{P}^*\Sigma_Q^*(^6P_{7/2}) \right). \quad (\text{A4})$$

The basis transformation is done by

$$\psi_{J^P}^{\text{LCS}} = U_{J^P}^{-1} \psi_{J^P}^{\text{HM}}. \quad (\text{A5})$$

The component of wave functions in LCS basis is

$$\psi_{1/2^+}^{\text{LCS}} = \begin{pmatrix} \left[ \begin{array}{l} [\bar{Q}Q]_0 [P[q[d]_{11/2}]_{1/2}] \\ [\bar{Q}Q]_0 [P[q[d]_{13/2}]_{1/2}] \\ [\bar{Q}Q]_1 [P[q[d]_{11/2}]_{1/2}] \\ [\bar{Q}Q]_1 [P[q[d]_{13/2}]_{1/2}] \\ [\bar{Q}Q]_1 [P[q[d]_{11/2}]_{3/2}] \\ [\bar{Q}Q]_1 [P[q[d]_{13/2}]_{3/2}] \end{array} \right] \begin{array}{l} \text{singlet-1} \\ \text{singlet-2} \\ \text{doublet-1} \\ \text{doublet-2} \\ \text{triplet-1} \\ \text{triplet-2} \end{array} \end{pmatrix}, \quad (\text{A6})$$

$$\psi_{3/2^+}^{\text{LCS}} = \begin{pmatrix} \left[ \begin{array}{l} [\bar{Q}Q]_0 [P[q[d]_{11/2}]_{3/2}] \\ [\bar{Q}Q]_0 [P[q[d]_{13/2}]_{3/2}] \\ [\bar{Q}Q]_1 [P[q[d]_{11/2}]_{1/2}] \\ [\bar{Q}Q]_1 [P[q[d]_{13/2}]_{1/2}] \\ [\bar{Q}Q]_1 [P[q[d]_{11/2}]_{3/2}] \\ [\bar{Q}Q]_1 [P[q[d]_{13/2}]_{3/2}] \\ [\bar{Q}Q]_1 [P[q[d]_{13/2}]_{5/2}] \end{array} \right] \begin{array}{l} \text{singlet-3} \\ \text{singlet-4} \\ \text{doublet-1} \\ \text{doublet-2} \\ \text{triplet-1} \\ \text{triplet-2} \\ \text{triplet-3} \end{array} \end{pmatrix}, \quad (\text{A7})$$

$$\psi_{5/2^+}^{\text{LCS}} = \begin{pmatrix} \left[ \begin{array}{c} [\bar{Q}Q]_0 [P[q[d]_1]_{3/2}]_{5/2} \\ \text{singlet-5} \end{array} \right]_{5/2} \\ \left[ \begin{array}{c} [\bar{Q}Q]_1 [P[q[d]_1]_{1/2}]_{3/2} \\ \text{triplet-1} \end{array} \right]_{5/2} \\ \left[ \begin{array}{c} [\bar{Q}Q]_1 [P[q[d]_1]_{3/2}]_{3/2} \\ \text{triplet-2} \end{array} \right]_{5/2} \\ \left[ \begin{array}{c} [\bar{Q}Q]_1 [P[q[d]_1]_{3/2}]_{5/2} \\ \text{triplet-3} \end{array} \right]_{5/2} \end{pmatrix}, \quad (\text{A8})$$

$$\psi_{7/2^+}^{\text{LCS}} = \left( \left[ \begin{array}{c} [\bar{Q}Q]_1 [P[q[d]_1]_{3/2}]_{5/2} \\ \text{triplet-3} \end{array} \right]_{7/2} \right). \quad (\text{A9})$$

The notation of spin structure is same with in Sec.II. The transformation matrix  $U$  is determined by the Clebsch-Gordan coefficient to reconstruct the spin structures from HM basis to LCS basis.

$$U_{1/2^+} = \begin{pmatrix} \frac{1}{2} & 0 & \frac{\sqrt{3}}{18} & \frac{2\sqrt{6}}{9} & \frac{\sqrt{6}}{9} & \frac{\sqrt{30}}{9} \\ 0 & \frac{1}{2} & \frac{2\sqrt{6}}{9} & \frac{5\sqrt{3}}{18} & -\frac{\sqrt{3}}{9} & -\frac{\sqrt{15}}{9} \\ -\frac{\sqrt{3}}{6} & 0 & -\frac{5}{18} & \frac{2\sqrt{2}}{9} & -\frac{5\sqrt{2}}{9} & \frac{\sqrt{10}}{9} \\ 0 & -\frac{\sqrt{3}}{3} & -\frac{2\sqrt{2}}{9} & \frac{5}{9} & \frac{1}{9} & -\frac{2\sqrt{5}}{9} \\ \frac{\sqrt{6}}{3} & 0 & -\frac{\sqrt{2}}{9} & -\frac{2}{9} & -\frac{4}{9} & -\frac{\sqrt{5}}{9} \\ 0 & \frac{\sqrt{15}}{6} & -\frac{2\sqrt{10}}{9} & \frac{\sqrt{5}}{18} & \frac{\sqrt{5}}{9} & -\frac{1}{9} \end{pmatrix}, \quad (\text{A10})$$

$$U_{3/2^+} = \begin{pmatrix} \frac{1}{2} & 0 & -\frac{\sqrt{3}}{9} & \frac{\sqrt{6}}{18} & -\frac{\sqrt{15}}{18} & \frac{2\sqrt{3}}{9} & \frac{\sqrt{2}}{2} \\ 0 & \frac{1}{2} & -\frac{\sqrt{15}}{9} & \frac{\sqrt{30}}{18} & \frac{2\sqrt{3}}{9} & \frac{11\sqrt{15}}{90} & -\frac{\sqrt{10}}{10} \\ -\frac{\sqrt{3}}{6} & 0 & \frac{5}{9} & \frac{\sqrt{2}}{18} & \frac{5\sqrt{5}}{18} & \frac{2}{9} & \frac{\sqrt{6}}{6} \\ 0 & -\frac{\sqrt{3}}{3} & \frac{\sqrt{5}}{9} & \frac{\sqrt{10}}{9} & -\frac{2}{9} & \frac{11\sqrt{5}}{45} & -\frac{\sqrt{30}}{15} \\ \frac{\sqrt{6}}{3} & 0 & \frac{2\sqrt{2}}{9} & -\frac{1}{18} & \frac{\sqrt{10}}{9} & -\frac{\sqrt{2}}{9} & -\frac{\sqrt{3}}{6} \\ 0 & \frac{\sqrt{15}}{6} & \frac{5}{9} & \frac{\sqrt{2}}{18} & -\frac{2\sqrt{5}}{9} & \frac{11}{90} & -\frac{\sqrt{6}}{30} \\ 0 & 0 & 0 & \frac{\sqrt{3}}{2} & 0 & -\frac{\sqrt{6}}{5} & \frac{1}{10} \end{pmatrix}, \quad (\text{A11})$$

$$U_{5/2^+} = \begin{pmatrix} \frac{1}{2} & -\frac{\sqrt{3}}{3} & \frac{\sqrt{15}}{15} & \frac{\sqrt{35}}{10} \\ -\frac{\sqrt{3}}{3} & \frac{1}{3} & \frac{2\sqrt{5}}{15} & \frac{\sqrt{105}}{15} \\ \frac{\sqrt{15}}{6} & \frac{\sqrt{5}}{3} & \frac{1}{15} & \frac{\sqrt{21}}{30} \\ 0 & 0 & \frac{\sqrt{21}}{5} & -\frac{2}{5} \end{pmatrix}, \quad (\text{A12})$$

$$U_{7/2^+} = 1. \quad (\text{A13})$$

In Sec.III we construct the one-pion exchange potential from the heavy hadron effective Lagrangians in HM basis. The detail of the OPEP matrix in HM basis is as follows :

$$V_{1/2^+}^{\text{HM}} = \begin{pmatrix} 0 & 0 & -\frac{\sqrt{3}}{3}C & \frac{\sqrt{6}}{3}T & \frac{\sqrt{6}}{6}C & \frac{\sqrt{30}}{30}T \\ 0 & 0 & \frac{\sqrt{6}}{6}T & -\frac{\sqrt{3}}{6}C - \frac{\sqrt{3}}{6}T & -\frac{\sqrt{3}}{6}T & -\frac{\sqrt{15}}{6}C + \frac{2\sqrt{15}}{15}T \\ -\frac{\sqrt{3}}{3}C & \frac{\sqrt{6}}{6}T & \frac{2}{3}C & \frac{\sqrt{2}}{3}T & \frac{\sqrt{2}}{6}C & \frac{2\sqrt{10}}{15}T \\ \frac{\sqrt{6}}{3}T & -\frac{\sqrt{3}}{6}C - \frac{\sqrt{3}}{6}T & \frac{\sqrt{2}}{3}T & -\frac{1}{3}C + \frac{2}{3}T & \frac{1}{6}T & \frac{\sqrt{5}}{6}C - \frac{\sqrt{5}}{30}T \\ \frac{\sqrt{6}}{6}C & -\frac{\sqrt{3}}{6}T & \frac{\sqrt{2}}{6}C & \frac{1}{6}T & \frac{5}{6}C & -\frac{7\sqrt{5}}{30}T \\ \frac{\sqrt{30}}{30}T & -\frac{\sqrt{15}}{6}C + \frac{2\sqrt{15}}{15}T & \frac{2\sqrt{10}}{15}T & \frac{\sqrt{5}}{6}C - \frac{\sqrt{5}}{30}T & -\frac{7\sqrt{5}}{30}T & \frac{1}{3}C + \frac{8}{15}T \end{pmatrix} \frac{gg_1}{f_\pi^2}, \quad (\text{A14})$$

$$V_{3/2^+}^{\text{HM}} = \begin{pmatrix} 0 & 0 & -\frac{\sqrt{3}}{3}C & -\frac{\sqrt{15}}{15}T & \frac{\sqrt{6}}{6}C & -\frac{\sqrt{3}}{30}T & \frac{3\sqrt{2}}{10}T \\ 0 & 0 & -\frac{\sqrt{15}}{30}T & -\frac{\sqrt{3}}{6}C + \frac{2\sqrt{3}}{15}T & \frac{\sqrt{30}}{60}T & -\frac{\sqrt{15}}{6}C - \frac{8\sqrt{15}}{75}T & \frac{21\sqrt{10}}{100}T \\ -\frac{\sqrt{3}}{3}C & -\frac{\sqrt{15}}{30}T & \frac{2}{3}C & -\frac{\sqrt{5}}{15}T & \frac{\sqrt{2}}{6}C & -\frac{2}{15}T & -\frac{\sqrt{6}}{10}T \\ -\frac{\sqrt{15}}{15}T & -\frac{\sqrt{3}}{6}C + \frac{2\sqrt{3}}{15}T & -\frac{\sqrt{5}}{15}T & -\frac{1}{3}C - \frac{8}{15}T & -\frac{\sqrt{10}}{60}T & \frac{\sqrt{5}}{6}C + \frac{2\sqrt{5}}{75}T & \frac{7\sqrt{30}}{100}T \\ \frac{\sqrt{6}}{6}C & \frac{\sqrt{30}}{60}T & \frac{\sqrt{2}}{6}C & -\frac{\sqrt{10}}{60}T & \frac{5}{6}C & \frac{7\sqrt{2}}{60}T & -\frac{\sqrt{3}}{5}T \\ -\frac{\sqrt{3}}{30}T & -\frac{\sqrt{15}}{6}C - \frac{8\sqrt{15}}{75}T & -\frac{2}{15}T & \frac{\sqrt{5}}{6}C + \frac{2\sqrt{5}}{75}T & \frac{7\sqrt{2}}{60}T & \frac{1}{3}C - \frac{32}{75}T & -\frac{7\sqrt{6}}{100}T \\ \frac{3\sqrt{2}}{10}T & \frac{21\sqrt{10}}{100}T & -\frac{\sqrt{6}}{10}T & \frac{7\sqrt{30}}{100}T & -\frac{\sqrt{3}}{5}T & -\frac{7\sqrt{6}}{100}T & -\frac{1}{2}C + \frac{14}{25}T \end{pmatrix} \frac{gg_1}{f_\pi^2}, \quad (\text{A15})$$

$$V_{5/2^+}^{\text{HM}} = \begin{pmatrix} 0 & -\frac{\sqrt{3}}{6}C - \frac{\sqrt{3}}{30}T & -\frac{\sqrt{3}}{6}C - \frac{\sqrt{3}}{30}T & -\frac{\sqrt{15}}{6}C + \frac{2\sqrt{15}}{75}T & -\frac{3\sqrt{35}}{50}T \\ -\frac{\sqrt{3}}{6}C - \frac{\sqrt{3}}{30}T & -\frac{1}{3}C + \frac{2}{15}T & -\frac{1}{3}C + \frac{2}{15}T & \frac{\sqrt{5}}{6}C - \frac{\sqrt{5}}{150}T & -\frac{\sqrt{105}}{50}T \\ -\frac{\sqrt{15}}{6}C + \frac{2\sqrt{15}}{75}T & \frac{\sqrt{5}}{6}C - \frac{\sqrt{5}}{150}T & \frac{\sqrt{5}}{6}C - \frac{\sqrt{5}}{150}T & \frac{1}{3}C + \frac{8}{75}T & \frac{\sqrt{21}}{50}T \\ -\frac{3\sqrt{35}}{50}T & -\frac{\sqrt{105}}{50}T & -\frac{\sqrt{105}}{50}T & \frac{\sqrt{21}}{50}T & -\frac{1}{2}C - \frac{16}{25}T \end{pmatrix} \frac{gg_1}{f_\pi^2}, \quad (\text{A16})$$

$$V_{7/2^+}^{\text{HM}} = \frac{gg_1}{f_\pi^2} \left[ -\frac{1}{2}C + \frac{1}{5}T \right]. \quad (\text{A17})$$

The definition of the spin-spin potential  $C$  and tensor potential  $T$  are written in Sec.III. The transformation of potential matrix from HM basis to LCS basis is done by

$$V_{J^P}^{\text{LCS}} = U_{J^P}^{-1} V_{J^P}^{\text{HM}} U_{J^P}. \quad (\text{A18})$$

The potential matrices in LCS basis are written in Sec.III.

The kinetic term is defined by

$$K_i^L = -\frac{1}{2\mu_i} \left( \frac{\partial^2}{\partial r^2} + \frac{2}{r} \frac{\partial}{\partial r} - \frac{L(L+1)}{r^2} \right), \quad (\text{A19})$$

where  $i$  is a channel index,  $L$  is an orbital angular momentum, and  $\mu_i$  is a reduced mass of channel  $i$ . The kinetic term matrices for each  $J^P$  in HM basis are as

follows :

$$K_{1/2^+}^{\text{HM}} = \text{diag} \left[ K_{\bar{P}\Sigma_Q}^1, K_{\bar{P}\Sigma_Q^*}^1, K_{\bar{P}^*\Sigma_Q}^1, K_{\bar{P}^*\Sigma_Q}^1, K_{\bar{P}^*\Sigma_Q^*}^1, K_{\bar{P}^*\Sigma_Q^*}^1 \right], \quad (\text{A20})$$

$$K_{3/2^+}^{\text{HM}} = \text{diag} \left[ K_{\bar{P}\Sigma_Q}^1, K_{\bar{P}\Sigma_Q^*}^1, K_{\bar{P}^*\Sigma_Q}^1, K_{\bar{P}^*\Sigma_Q}^1, K_{\bar{P}^*\Sigma_Q^*}^1, K_{\bar{P}^*\Sigma_Q^*}^1 \right], \quad (\text{A21})$$

$$K_{5/2^+}^{\text{HM}} = \text{diag} \left[ K_{\bar{P}\Sigma_Q^*}^1, K_{\bar{P}^*\Sigma_Q}^1, K_{\bar{P}^*\Sigma_Q^*}^1, K_{\bar{P}^*\Sigma_Q^*}^1 \right], \quad (\text{A22})$$

$$K_{7/2^+}^{\text{HM}} = K_{\bar{P}^*\Sigma_Q^*}^1. \quad (\text{A23})$$

The transformation to LCS basis is done by

$$K_{J^P}^{\text{LCS}} = U_{J^P}^{-1} K_{J^P}^{\text{HM}} U_{J^P}. \quad (\text{A24})$$

- 
- [1] R. Aaij *et al.* [LHCb Collaboration], Observation of  $J/\psi p$  Resonances Consistent with Pentaquark States in  $\Lambda_b^0 \rightarrow J/\psi K^- p$  Decays, Phys. Rev. Lett. **115**, 072001 (2015).
- [2] R. Aaij *et al.* [LHCb Collaboration], Model-independent evidence for  $J/\psi p$  contributions to  $\Lambda_b^0 \rightarrow J/\psi p K^-$  decays, Phys. Rev. Lett. **117**, no. 8, 082002 (2016).
- [3] R. Aaij *et al.* [LHCb Collaboration], Evidence for exotic hadron contributions to  $\Lambda_b^0 \rightarrow J/\psi p \pi^-$  decays, Phys. Rev. Lett. **117**, no. 8, 082003 (2016).
- [4] J. J. Wu, R. Molina, E. Oset and B. S. Zou, Prediction of narrow  $N^*$  and  $\Lambda^*$  resonances with hidden charm above 4 GeV, Phys. Rev. Lett. **105**, 232001 (2010).
- [5] Z. C. Yang, Z. F. Sun, J. He, X. Liu and S. L. Zhu, The possible hidden-charm molecular baryons composed of anti-charmed meson and charmed baryon, Chin. Phys. C **36**, 6 (2012).
- [6] W. L. Wang, F. Huang, Z. Y. Zhang and B. S. Zou,  $\Sigma_c \bar{D}$  and  $\Lambda_c \bar{D}$  states in a chiral quark model, Phys. Rev. C **84**, 015203 (2011).
- [7] J. J. Wu, T.-S. H. Lee and B. S. Zou, Nucleon Resonances with Hidden Charm in Coupled-Channel Models, Phys. Rev. C **85**, 044002 (2012).
- [8] R. Chen, X. Liu, X. Q. Li and S. L. Zhu, Identifying exotic hidden-charm pentaquarks, Phys. Rev. Lett. **115**, no. 13, 132002 (2015).
- [9] J. He,  $\bar{D}\Sigma_c^*$  and  $\bar{D}^*\Sigma_c$  interactions and the LHCb hidden-charmed pentaquarks, Phys. Lett. B **753**, 547 (2016).
- [10] H. X. Chen, W. Chen, X. Liu, T. G. Steele and S. L. Zhu, Towards exotic hidden-charm pentaquarks in QCD, Phys. Rev. Lett. **115**, no. 17, 172001 (2015).
- [11] H. Huang, C. Deng, J. Ping and F. Wang, Possible pentaquarks with heavy quarks, Eur. Phys. J. C **76**, no. 11, 624 (2016).
- [12] L. Roca, J. Nieves and E. Oset, LHCb pentaquark as a  $\bar{D}^*\Sigma_c - \bar{D}^*\Sigma_c^*$  molecular state, Phys. Rev. D **92**, no. 9, 094003 (2015).
- [13] U. G. Meißner and J. A. Oller, Testing the  $\chi_{c1} p$  composite nature of the  $P_c(4450)$ , Phys. Lett. B **751**, 59 (2015).
- [14] C. W. Xiao and U.-G. Meißner,  $J/\psi(\eta_c)N$  and  $\Upsilon(\eta_b)N$  cross sections, Phys. Rev. D **92**, no. 11, 114002 (2015).

- [15] T. J. Burns, Phenomenology of  $P_c(4380)^+$ ,  $P_c(4450)^+$  and related states, *Eur. Phys. J. A* **51**, no. 11, 152 (2015).
- [16] D. E. Kahana and S. H. Kahana, LHCb  $P_c^+$  Resonances as Molecular States, arXiv:1512.01902 [hep-ph].
- [17] H. X. Chen, E. L. Cui, W. Chen, X. Liu, T. G. Steele and S. L. Zhu, QCD sum rule study of hidden-charm pentaquarks, *Eur. Phys. J. C* **76**, no. 10, 572 (2016).
- [18] Y. Shimizu, D. Suenaga and M. Harada, Coupled channel analysis of molecule picture of  $P_c(4380)$ , *Phys. Rev. D* **93**, no. 11, 114003 (2016).
- [19] Y. Yamaguchi and E. Santopinto, Hidden-charm pentaquarks as a meson-baryon molecule with coupled channels for  $\bar{D}^{(*)}\Lambda_c$  and  $\bar{D}^{(*)}\Sigma_c^{(*)}$ , *Phys. Rev. D* **96**, no. 1, 014018 (2017).
- [20] J. He, Understanding spin parity of  $P_c(4450)$  and  $Y(4274)$  in a hadronic molecular state picture, *Phys. Rev. D* **95**, no. 7, 074004 (2017).
- [21] P. G. Ortega, D. R. Entem and F. Fernández, LHCb pentaquarks in constituent quark models, *Phys. Lett. B* **764**, 207 (2017).
- [22] K. Azizi, Y. Sarac and H. Sundu, Analysis of  $P_c^+(4380)$  and  $P_c^+(4450)$  as pentaquark states in the molecular picture with QCD sum rules, *Phys. Rev. D* **95**, no. 9, 094016 (2017).
- [23] L. Geng, J. Lu and M. P. Valderrama, Scale Invariance in Heavy Hadron Molecules, arXiv:1704.06123 [hep-ph].
- [24] E. Santopinto and A. Giachino, Compact pentaquark structures, *Phys. Rev. D* **96**, no. 1, 014014 (2017).
- [25] J. Wu, Y. R. Liu, K. Chen, X. Liu and S. L. Zhu, Hidden-charm pentaquarks and their hidden-bottom and  $B_c$ -like partner states, *Phys. Rev. D* **95**, no. 3, 034002 (2017).
- [26] E. Hiyama, A. Hosaka, M. Oka and J. M. Richard, Quark model estimate of hidden-charm pentaquark resonances, *Phys. Rev. C* **98**, no. 4, 045208 (2018).
- [27] L. Maiani, A. D. Polosa and V. Riquer, The New Pentaquarks in the Diquark Model, *Phys. Lett. B* **749**, 289 (2015).
- [28] R. F. Lebed, The Pentaquark Candidates in the Dynamical Diquark Picture, *Phys. Lett. B* **749**, 454 (2015).
- [29] G. N. Li, X. G. He and M. He, Some Predictions of Diquark Model for Hidden Charm Pentaquark Discovered at the LHCb, *JHEP* **1512**, 128 (2015).
- [30] Z. G. Wang, Analysis of  $P_c(4380)$  and  $P_c(4450)$  as pentaquark states in the diquark model with QCD sum rules, *Eur. Phys. J. C* **76**, no. 2, 70 (2016).
- [31] R. Zhu and C. F. Qiao, Pentaquark states in a diquark-triquark model, *Phys. Lett. B* **756**, 259 (2016).
- [32] S. Takeuchi and M. Takizawa, The hidden charm pentaquarks are the hidden color-octet  $uud$  baryons?, *Phys. Lett. B* **764**, 254 (2017).
- [33] V. Kubarovsky and M. B. Voloshin, Formation of hidden-charm pentaquarks in photon-nucleon collisions, *Phys. Rev. D* **92**, no. 3, 031502 (2015).
- [34] M. I. Eides, V. Y. Petrov and M. V. Polyakov, Pentaquarks with hidden charm as hadroquarkonia, *Eur. Phys. J. C* **78**, no. 1, 36 (2018).
- [35] N. N. Scoccola, D. O. Riska and M. Rho, Pentaquark candidates  $P_c^+(4380)$  and  $P_c^+(4450)$  within the soliton picture of baryons, *Phys. Rev. D* **92**, no. 5, 051501 (2015).
- [36] Y. Liu and I. Zahed, "Heavy and Strange Holographic Baryons," *Phys. Rev. D* **96**, no. 5, 056027 (2017).
- [37] Y. Yamaguchi, A. Giachino, A. Hosaka, E. Santopinto, S. Takeuchi and M. Takizawa, Hidden-charm and bottom meson-baryon molecules coupled with five-quark states, *Phys. Rev. D* **96**, no. 11, 114031 (2017).
- [38] H. X. Chen, W. Chen, X. Liu and S. L. Zhu, "The hidden-charm pentaquark and tetraquark states," *Phys. Rept.* **639**, 1 (2016).
- [39] A. Ali, J. S. Lange and S. Stone, "Exotics: Heavy Pentaquarks and Tetraquarks," *Prog. Part. Nucl. Phys.* **97**, 123 (2017).
- [40] F. K. Guo, C. Hanhart, U. G. Meiner, Q. Wang, Q. Zhao and B. S. Zou, "Hadronic molecules," *Rev. Mod. Phys.* **90**, no. 1, 015004 (2018).
- [41] N. Isgur and M. B. Wise, Weak Decays of Heavy Mesons in the Static Quark Approximation, *Phys. Lett. B* **232** (1989) 113.
- [42] N. Isgur and M. B. Wise, Weak Transition Form-factors Between Heavy Mesons, *Phys. Lett. B* **237**, 527 (1990).
- [43] N. Isgur and M. B. Wise, Spectroscopy with heavy quark symmetry, *Phys. Rev. Lett.* **66** (1991) 1130.
- [44] M. Neubert, Heavy quark symmetry, *Phys. Rept.* **245**, 259 (1994).
- [45] A. V. Manohar and M. B. Wise, *Heavy Quark Physics*, (Cambridge University Press, Cambridge, 2000)
- [46] S. Yasui, K. Sudoh, Y. Yamaguchi, S. Ohkoda, A. Hosaka and T. Hyodo, Spin degeneracy in multi-hadron systems with a heavy quark, *Phys. Lett. B* **727**, 185 (2013).
- [47] Y. Yamaguchi, S. Ohkoda, A. Hosaka, T. Hyodo and S. Yasui, Heavy quark symmetry in multihadron systems, *Phys. Rev. D* **91**, 034034 (2015).
- [48] A. Hosaka, T. Hyodo, K. Sudoh, Y. Yamaguchi and S. Yasui, Heavy Hadrons in Nuclear Matter, *Prog. Part. Nucl. Phys.* **96**, 88 (2017).
- [49] Y. Shimizu, Y. Yamaguchi and M. Harada, "Heavy quark spin multiplet structure of  $\bar{P}^{(*)}\Sigma_Q^{(*)}$  molecular states," *Phys. Rev. D* **98**, no. 1, 014021 (2018).
- [50] A. F. Falk, Hadrons of arbitrary spin in the heavy quark effective theory, *Nucl. Phys. B* **378**, 79 (1992).
- [51] M. B. Wise, Chiral perturbation theory for hadrons containing a heavy quark, *Phys. Rev. D* **45**, no. 7, R2188 (1992).
- [52] P. L. Cho, Chiral perturbation theory for hadrons containing a heavy quark: The Sequel, *Phys. Lett. B* **285**, 145 (1992).
- [53] T. M. Yan, H. Y. Cheng, C. Y. Cheung, G. L. Lin, Y. C. Lin and H. L. Yu, Heavy quark symmetry and chiral dynamics, *Phys. Rev. D* **46**, 1148 (1992) Erratum: [*Phys. Rev. D* **55**, 5851 (1997)].
- [54] A. F. Falk and M. E. Luke, Strong decays of excited heavy mesons in chiral perturbation theory, *Phys. Lett. B* **292**, 119 (1992).
- [55] Y. R. Liu and M. Oka,  $\Lambda_c N$  bound states revisited, *Phys. Rev. D* **85**, 014015 (2012).
- [56] A. Bohr and B. R. Mottelson, *Nuclear Structure*, Vol. I, (W. A. Benjamin, Inc., New York, 1969)
- [57] C. Patrignani *et al.* [Particle Data Group], Review of Particle Physics, *Chin. Phys. C* **40**, no. 10, 100001 (2016).
- [58] E. Hiyama, Y. Kino and M. Kamimura, Gaussian expansion method for few-body systems, *Prog. Part. Nucl. Phys.* **51**, 223 (2003).
- [59] F. K. Guo, U. G. Meißner, W. Wang and Z. Yang, How to reveal the exotic nature of the  $P_c(4450)$ , *Phys. Rev. D* **92**, no. 7, 071502 (2015).
- [60] X. H. Liu, Q. Wang and Q. Zhao, Understanding the newly observed heavy pentaquark candidates, *Phys. Lett.*

- B **757**, 231 (2016).
- [61] F. K. Guo, U. G. Meißner, J. Nieves and Z. Yang, Remarks on the  $P_c$  structures and triangle singularities, Eur. Phys. J. A **52**, no. 10, 318 (2016).
- [62] M. Bayar, F. Aceti, F. K. Guo and E. Oset, A Discussion on Triangle Singularities in the  $\Lambda_b \rightarrow J/\psi K^- p$  Reaction, Phys. Rev. D **94**, no. 7, 074039 (2016).